

PACS numbers: 71.15.Mb, 71.20.-b, 78.30.-j, 78.40.-q, 78.67.Sc, 81.07.Pr, 82.35.Np

## Design and Augmentation of the Optical and Electronic Characteristics of BaTiO<sub>3</sub>-Nanostructures-Doped PVA/PEG for Electronics Nanodevices

Batool Mohammed, Hind Ahmed, and Ahmed Hashim

*College of Education for Pure Sciences,  
Department of Physics,  
University of Babylon,  
Hillah, Iraq*

The present work aims to design of PVA/PEG/BaTiO<sub>3</sub> nanostructures and investigating the structural, electronic, optical and thermal properties to use in future optics and electronics applications. The designed nanostructures have individual properties including low cost, lightweight, high corrosion resistance and good optical and electronic characteristics in comparison with other nanostructures. Using DFT with the hybrid functional B3LYP, the characteristics of PVA/PEG/BaTiO<sub>3</sub> nanostructures are studied. The electronic characteristics include total energy, energies of HOMO and LUMO, ionization energy, energy gap, electronegativity, electron affinity, electronic softness, electrophilic index, electron density, electrostatic potential, density of states, dipole moment, polarizability, and IR-spectra. The thermal properties include thermal energy, enthalpy, specific heat, and entropy. The optical properties include the UV-spectra. The results indicate that the PVA/PEG/BaTiO<sub>3</sub> nanostructures have energy gap equal to 1.705 eV with good optical, thermal and electronic properties, which make it be useful in the electronics and optics fields.

Дану роботу спрямовано на проектування наноструктур полівінілалкоголь/поліетиленгліколь/ВаТіО<sub>3</sub> (PVA/PEG/BaTiO<sub>3</sub>) та дослідження структурних, електронних, оптичних і теплових властивостей для використання в майбутній оптиці й електроніці. Спроектвані наноструктури мають індивідуальні властивості, включаючи низьку вартість, легкість, високу корозійну стійкість і хороші оптичні й електронні характеристики в порівнянні з іншими наноструктурами. Використовуючи теорію функціоналу густини з гібридним функціоналом B3LYP, досліджено характеристики наноструктур PVA/PEG/BaTiO<sub>3</sub>. Електронні характеристики включають повну енергію, енергії HOMO та LUMO, енергію йонізації, енергетичну щільність, електронегативність, спорідненість до електронів, електронну м'якість, індекс електрофільності, елект-

ронну густину, електростатичний потенціал, густину станів, дипольний момент, поляризацію й ІЧ-спектри. Теплові властивості включають теплову енергію, ентальпію, питоме тепло й ентропію. До оптичних властивостей відносяться УФ-спектри. Результати показують, що наноструктури PVA/PEG/BaTiO<sub>3</sub> мають енергетичну щілину, що дорівнює 1,705 eV, з хорошими оптичними, тепловими й електронними властивостями, що робить їх корисними в областях електроніки й оптики.

**Key words:** BaTiO<sub>3</sub>, DFT, energy gap, optical properties, polymer, electronics applications.

**Ключові слова:** BaTiO<sub>3</sub>, ТФГ, енергетична щілина, оптичні властивості, полімер, застосування електроніки.

*(Received 14 May, 2022)*

## 1. INTRODUCTION

Inorganic–organic nanocomposites have gained a scientific robust in the approaches of optics (linear and nonlinear) and solar cells owing to their exceptional characteristics and new applications. Combining one or more nanoparticles of metal oxide with one or more polymer leads to a novel type of state-of-the-art nanocomposites. Mostly, the incorporation of metal oxide and polymers has been exhibited to nanocomposites manifesting good electrical, mechanical and optical characteristics. Polymer composites increased many striking characteristics like easy processing, resistance to deformations and organic functionalities [1]. Ferroelectric materials are distinguished by having a polarization direction that may be switched in response to an external electric field, which generates several technical fields [2].

Perovskite oxides like BaTiO<sub>3</sub> have good ferroelectric polarization and piezoelectricity characterizations, which allow many significant technology fields. Extensive studies have shown that these characterizations sensitively depend on external conditions like thickness, strain, interface structures [3]. Due to the good ferroelectric and piezoelectric characteristics, BaTiO<sub>3</sub> ceramic may be applied as an optically information processing materials or a photoelectric device materials relate to its sensitivity to light refraction and higher photoelectric coefficient [4].

Polyvinyl alcohol (PVA) can be blended with other polymers to form polymer complexes by hydrogen bonding. Hydroxyl groups, which are located on the carbon chain backbone of the polymer, are considered the main source of the hydrogen bonding. On the other hand, polyethylene glycol (PEG) is a highly water soluble and non-toxic material; besides, its solubility in most organic solvents is considerably high. Moreover, when PEG is mixed with other polymeric

material, most of these properties can be shared within the resulting blend [5]. The composites of polymer doped with inorganic material included many applications in electronics and optoelectronics [6–19].

Gaussian 03 program is computer software, which is capable predicting several characterizations of molecules and reactions, which are included the molecular energies and structures [20].

This work aims to design of new PVA/PEG/BaTiO<sub>3</sub> nanostructures combining between the properties of PVA/PEG blend and BaTiO<sub>3</sub> nanostructures to create new material used as a key for different electronics fields.

## 2. THEORETICAL PART

Energy gap refers to difference of the HOMO and LUMO levels [21]:

$$E_g = E_{\text{LUMO}} - E_{\text{HOMO}}.$$

The ionization energy is given by Ref. [22] as follows:  $I_E = -E_{\text{HOMO}}$ . Electron affinity is defined by the following equation [21]:

$$E_A = -E_{\text{LUMO}}.$$

The chemical potential is determined by the relation [23]:

$$\mu \approx (E_{\text{HOMO}} + E_{\text{LUMO}})/2 \approx -(I_E + E_A)/2.$$

Chemical hardness is given by Ref. [24] as follows:  $H = (I_E - E_A)/2$ .

Chemical softness is defined by the equation [25]:  $S = (2H)^{-1}$ .

Electrophilicity is given by the relation [25]:  $w = \mu^2/(2H)$ .

The electronegativity is determined by the equation [26]:

$$E_N = -(I_E + E_A)/2.$$

Polarizability is the linear response measure of the electron density in the presence of an infinitesimal electric field [27]. The polarizability is given by the equation [28]:  $\alpha_{ave} = (\alpha_{xx} + \alpha_{yy} + \alpha_{zz})/3$ .

## 3. RESULTS AND DISCUSSION

Figure 1 shows the found relaxation of the molecule, in which the optimized structure of the molecule is the structure at minimum energy, and it is performed by finding the first derivative of the energy with respect to distance between various atoms.

Table 1 represents the standard orientation of all atoms in the

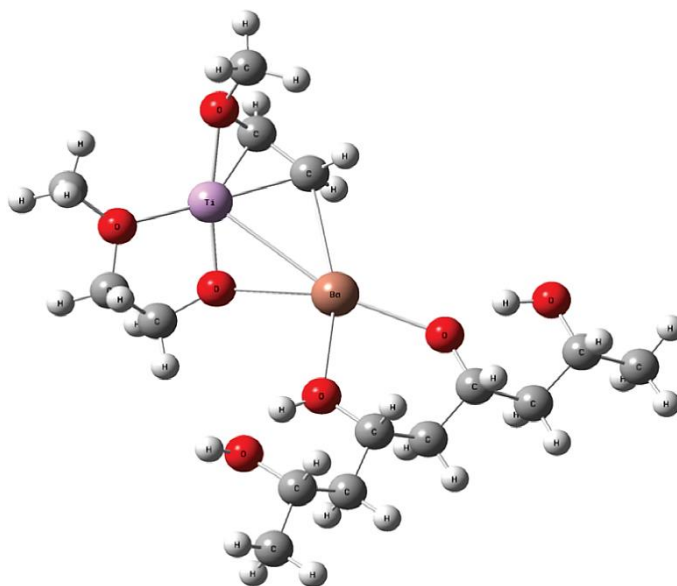


Fig. 1. Optimization of PVA/PEG/BaTiO<sub>3</sub> structures.

TABLE 1. Average lengths of bond and the angles.

Measurements	Optimization parameters	Values
Bonds, Å	(C–C)	1.541
	(C–O)	1.480
	(C–H)	1.098
	(O–H)	0.993
	(Ba–Ti)	3.482
	(Ti–O)	1.9736
	(Ba–O)	2.730
Angles, deg.	(C–C–C)	112.878
	(C–O–H)	109.132
	(Ba–O–Ti)	95.025

molecule. The bonds' values in present work are in a well agreement with Refs. [29, 30].

Figure 2 shows the IR spectrum of PVA/PEG/BaTiO<sub>3</sub> structures; using DFT, it has been found that the strong peak observed at 3000 cm<sup>-1</sup> is attributed to the (O–H) groups.

With Raman spectroscopy, a change is observed in the polarization of molecules, *i.e.*, the visible or ultraviolet photons interact with the vibrating molecular bonds, gaining or losing part of their

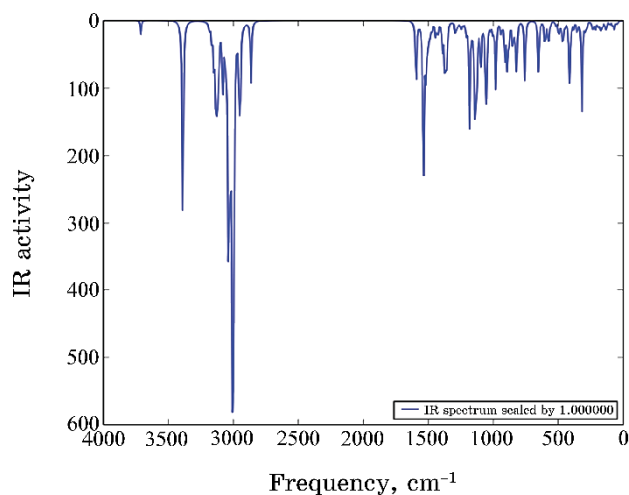


Fig. 2. IR spectra of PVA/PEG/BaTiO<sub>3</sub> structures.

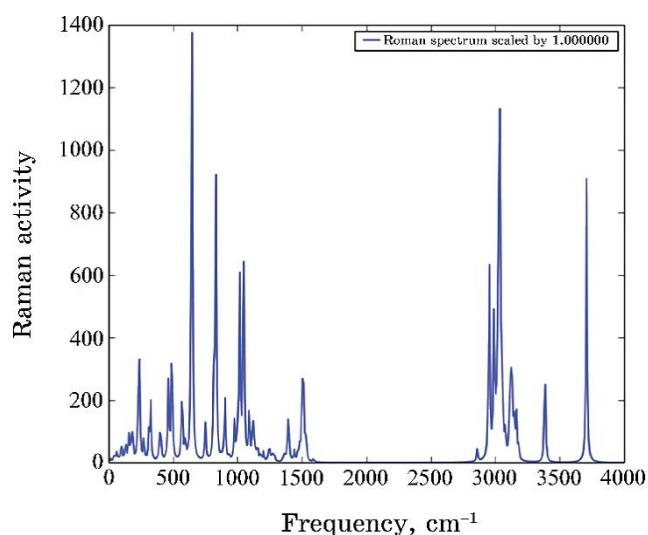


Fig. 3. Raman intensities of PVA/PEG/BaTiO<sub>3</sub> structures with vibration frequency.

energy, thereby, generating the spectrum [31].

Figure 3 shows the Raman spectra of PVA/PEG/BaTiO<sub>3</sub> structures. Intensities of Raman spectra depend on the probability that photon with particular wavelength will be absorbed.

Figure 4 show the UV-Vis spectra dependent on the molecule electronic structure. The UV-Vis-spectra calculations for the

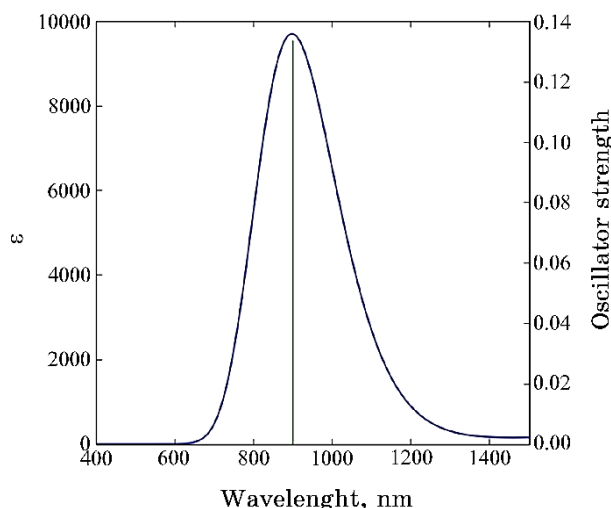


Fig. 4. UV-Vis spectrum for the PVA-PEG-BaTiO<sub>3</sub> composite.

TABLE 2. Energy-gap values of in [eV] for PVA/PEG/BaTiO<sub>3</sub> structures.

$E_{\text{HOMO}}$ , eV	$E_{\text{LUMO}}$ , eV	$E_g$ , eV
-2.262	-0.555	1.705

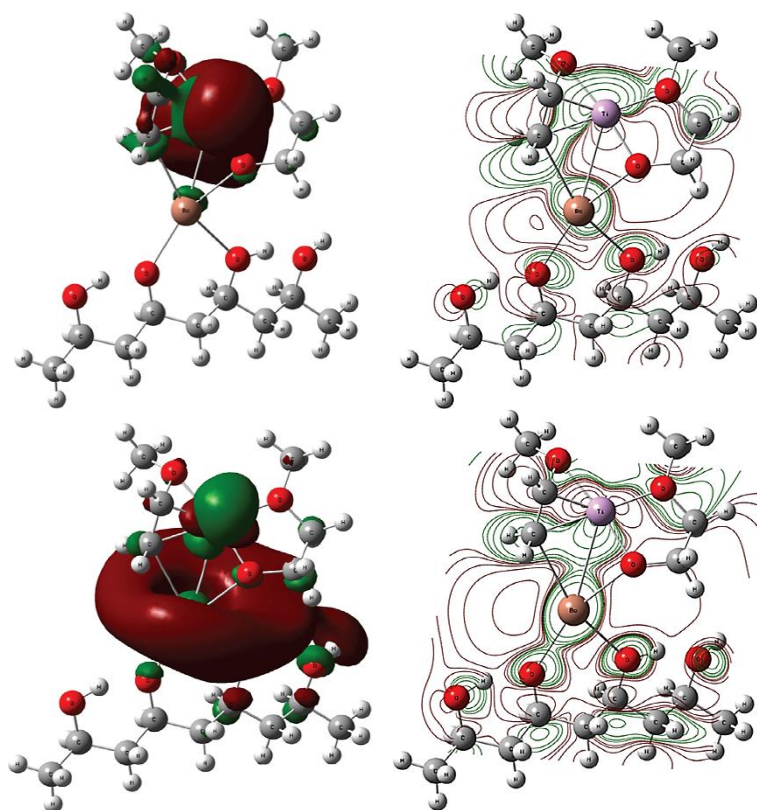
PVA/PEG/BaTiO<sub>3</sub> structures performed by means of the B3LYP-TD/LanL2DZ method include the excitation energy, wavelength, oscillator strength, and electronic transition.

Table 2 represents the energy gap of PVA/PEG/BaTiO<sub>3</sub> structures in comparison with Ref. [30].

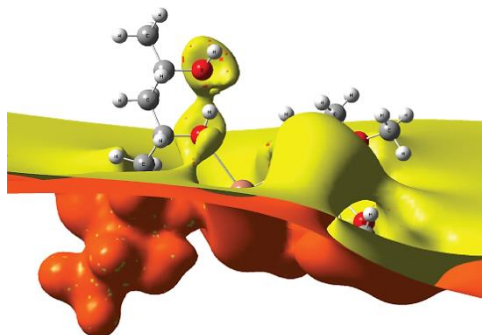
Figure 5 illustrates the 3D distribution of HOMO<sup>s</sup> and LUMO<sup>s</sup> for the studied structures.

Figure 6 illustrates the electrostatic surface potential (ESP) distribution for the PVA/PEG/BaTiO<sub>3</sub> structures calculated from the total self-consistent field approximation. ESP distributions of structures are caused by repulsive forces or by attracting regions around each structure. In general, the ESP distributions for the PVA/PEG/BaTiO<sub>3</sub> structures are dragged toward the negative-charges' positions in each molecule bases with high-electronegativity oxygen atoms (3.5 eV).

Table 3 shows the results of the ground state energy ( $E_T$ ) in [a.u.], the viral ratio ( $-V/T$ ) as the ratio of the negative magnitude of the potential energy to the kinetic energy, and some electronic characteristics of PVA/PEG/BaTiO<sub>3</sub> structures calculated at the same level of theory. These characteristics include  $I_E$ ,  $E_A$ ,  $E_N$ ,  $H$



**Fig. 5.** The distribution of HOMO (up row) and LUMO (down row) for the PVA/PEG/BaTiO<sub>3</sub> structures.



**Fig. 6.** Electrostatic-potential distribution surface for the PVA/PEG/BaTiO<sub>3</sub> structure.

and  $w$  [32].

**TABLE 3.** Electronic characteristics' values in [eV] for the structure.

Property	PVA/PEG/BaTiO <sub>3</sub> structures
Total energy	-1200.679 [a.u.]
Ionization potential	2.262
Electron affinity	0.555
Electronegativity	1.408
Chemical hardness	0.853
Chemical softness	0.585
Chemical potential	-1.408
Electrophilicity	3.383

**TABLE 4.** The polarizability of PVA/PEG/BaTiO<sub>3</sub> structures.

Polarizability, a.u.			
$\alpha_{xx}$ , a.u.	$\alpha_{yy}$ , a.u.	$\alpha_{zz}$ , a.u.	$\alpha_{ave}$ , a.u.
407.722	340.150	286.380	344.750

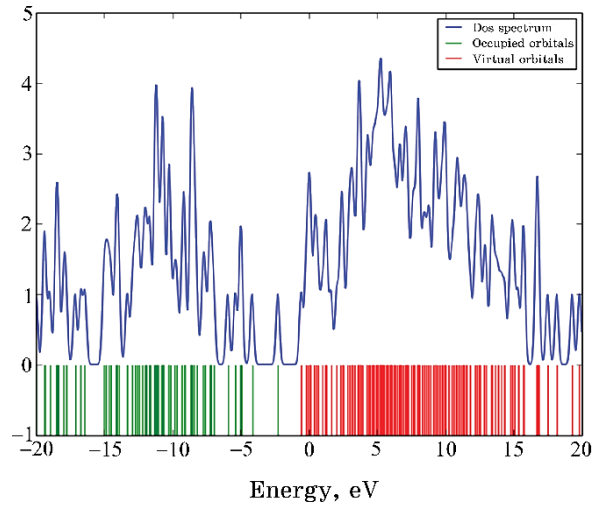
**Fig. 7.** DOS for the PVA/PEG/BaTiO<sub>3</sub> structures.

Table 4 shows the average polarizability ( $\alpha_{ave}$ ) and its components in [a.u.] of PVA/PEG/BaTiO<sub>3</sub> structures.

The density of states for the PVA/PEG/BaTiO<sub>3</sub> structures as a function of energy levels was calculated by employing the DFT-B3LYP/LanL2DZ level of theory. Figure 7 shows the degenerate states as functions of energy levels for the studied structure; this degeneracy is caused by the existence of the new types of atoms, and that leads to varying the bond lengths and angles or changing



**TABLE 5.**  $E_{th}$ ,  $c_v$  and  $S_{th}$  for the PVA/PEG/BaTiO<sub>3</sub> structures.

Thermal corrections (Hartree/Partial)			
	$E_{th}$ , kcal/mole	$c_v$ , cal/mole·K	$S_{th}$ , cal/mole·K
Electronic	0.000	0.000	1.377
Translational	0.889	2.981	44.575
Rotational	0.889	2.981	36.916
Vibrational	313.331	108.306	132.986
Total	315.109	114.268	214.477

the geometry of the structure.

Table 5 presents the thermal corrections of  $E_{th}$ ,  $c_v$  and  $S_{th}$  for the PVA/PEG/BaTiO<sub>3</sub> structures.

#### 4. CONCLUSIONS

In this work, design of new PVA/PEG/BaTiO<sub>3</sub> structures and studying the structure, electronic, optical and thermal properties have been made to use in various optics and electronics fields with good physical and chemical characteristics in comparison with other structures. The results show that good relaxation of the PVA/PEG/BaTiO<sub>3</sub> structures is obtained, using B3LYP-DFT at Gaussian 09 package of program. The ionization potential is greater than the electron affinity; so, these structures need high energy to become cation. The PVA/PEG/BaTiO<sub>3</sub> structures are more reactive according to the high level of the electrophilicity. Finally, the results indicate that the PVA/PEG/BaTiO<sub>3</sub> structures could be used in various optoelectronics fields.

#### REFERENCES

1. Q. M. Al-Bataineh, A. A. Ahmad, A. M. Alsaad, and A. D. Telfah, *Heliyon*, **7**: 1 (2021); <https://doi.org/10.1016/j.heliyon.2021.e05952>
2. M. E. Lines and A. M. Glass, *Principles and Applications of Ferroelectrics and Related Materials* (Oxford University Press: 2001).
3. Y. Duan, G. Tang, C. Chen, T. Lu, and Z. Wu, *Physical Review B*, **85**, No. 5: 054108 (2012); <https://doi.org/10.1103/PhysRevB.85.054108>
4. M. Yanan, C. Huanming, F. Pan, Z. Chen, Z. Ma, X. Lin, F. Zheng, and X. Ma, *Ceramics Int.*, **45**: 6303 (2019); <https://doi.org/10.1016/j.ceramint.2018.12.113>
5. A. A. Alhazime, *J. Inorg. Organomet. Polym.*, **30**: 4459 (2020); <https://doi.org/10.1007/s10904-020-01577-8>
6. W. Jilani, A. Jlali, and H. Guermazi, *Opt. Quant. Electron.*, **53**: 545 (2021); <https://doi.org/10.1007/s11082-021-03200-7>

7. N. Bano, I. Hussain, A. M. EL-Naggar, and A. A. Albassam, *Appl. Phys. A*, **125**: 1 (2019); <https://doi.org/10.1007/s00339-019-2518-8>
8. H. Ahmed and A. Hashim, *J. Mol. Model.*, **26**: 210 (2020); <https://doi.org/10.1007/s00894-020-04479-1>
9. A. Hazim, A. Hashim, and H. M. Abduljalil, *Trans. Electr. Electron. Mater.*, **21**: 48 (2019); <https://doi.org/10.1007/s42341-019-00148-0>
10. H. Ahmed and A. Hashim, *Trans. Electr. Electron. Mater.*, **23**: 237 (2021); <https://doi.org/10.1007/s42341-021-00340-1>
11. W. Jilani, A. Jlali, and H. Guerhazi, *Opt. Quant. Electron.*, **53**: 545 (2021); <https://doi.org/10.1007/s11082-021-03200-7>
12. H. Ahmed and A. Hashim, *Silicon*, **13**: 1509 (2021); <https://doi.org/10.1007/s12633-020-00543-w>
13. A. Hazim, H. M. Abduljalil, and A. Hashim, *Trans. Electr. Electron. Mater.*, **21**: 550 (2020); <https://doi.org/10.1007/s42341-020-00210-2>
14. H. Ahmed and A. Hashim, *Silicon*, **14**: 4907 (2022); <https://doi.org/10.1007/s12633-021-01258-2>
15. H. Ahmed and A. Hashim, *Silicon*, **13**: 2639 (2020); <https://doi.org/10.1007/s12633-020-00620-0>
16. A. Hazim, H. M. Abduljalil, and A. Hashim, *Trans. Electr. Electron. Mater.*, **22**: 185 (2020); <https://doi.org/10.1007/s42341-020-00224-w>
17. S. S. Alharthi, A. Alzahrani, M. A. N. Razvi et al., *J. Inorg. Organomet. Polym.*, **30**: 3878 (2020); <https://doi.org/10.1007/s10904-020-01519-4>
18. S. Kumar, S. Baruah, and A. Puzari, *Polym. Bull.*, **77**: 441 (2020); <https://doi.org/10.1007/s00289-019-02760-9>
19. J. Mohammed, T. T. Carol T., H. Y. Hafeez, D. Basandrai, G. R. Bhadu, S. K. Godara, S. B. Narang, and A. K. Srivastava, *J. Mater. Sci.: Mater. Electron.*, **30**: 4026 (2019); <https://doi.org/10.1007/s10854-019-00690-w>
20. M. J. Frisch and F. R. Clemente, *Gaussian 09, Revision A. 01* (M. J. Frisch, G. W. Trucks, H. B. Schlegel, G. E. Scuseria, M. A. Robb, J. R. Cheeseman, G. Scalmani, V. Barone, B. Mennucci, G. A. Petersson, H. Nakatsuji, M. Caricato, X. Li, H. P. Hratchian, A. F. Izmaylov, J. Bloino, G. Zhe).
21. H. M. Kampen, H. Méndez, and D. R. T. Zahn, *Technische Universität Chemnitz, Institut für Physik (Germany)* (1999); [https://www.tu-chemnitz.de/physik/HLPH/publications/p\\_src/438.pdf](https://www.tu-chemnitz.de/physik/HLPH/publications/p_src/438.pdf)
22. K. Sadasivam and R. Kumaresan, *Computational and Theoretical Chemistry*, **963**, No. 1: 227 (2011).
23. O. A. Kolawole and S. Banjo, *Theoretical Studies of Anti-Corrosion Properties of Triphenylimidazole Derivatives in Corrosion Inhibition of Carbon Steel in Acidic Media via DFT Approach*, **10**, No. 1: 136 (2018).
24. P. W. Atkins and R. S. Friedman, *Molecular Quantum Mechanics* (Oxford University Press: 2011); [http://sutlib2.sut.ac.th/sut\\_contents/H96900.pdf](http://sutlib2.sut.ac.th/sut_contents/H96900.pdf)
25. V. Subramanian, *Quantum Chemical Descriptors in Computational Medicinal Chemistry for Chemoinformatics*, Central Leather Research Institute, Chemical Laboratory (2005); [https://scholar.google.com/scholar?hl=ar&as\\_sdt=0%2C5&q=Subramanian%2C+V.+%282005%29.+Quantum+Chemical+Descriptors+in+Computational+Medicinal+Chemistry+for+Chemoinformatics.+Central+Leather+Research+Institute%2C+Chemical+Laboratory%2C+0-0000&btnG=](https://scholar.google.com/scholar?hl=ar&as_sdt=0%2C5&q=Subramanian%2C+V.+%282005%29.+Quantum+Chemical+Descriptors+in+Computational+Medicinal+Chemistry+for+Chemoinformatics.+Central+Leather+Research+Institute%2C+Chemical+Laboratory%2C+0-0000&btnG=)
26. L. Shenghua, Y. He, and J. Yuansheng, *Inter. J. of Molecul. Sci.*, **5**, No. 1:

- 13 (2004); <https://doi.org/10.3390/i5010013>
27. Ademir J. Camargo, Káthia M. Honyrio, Ricardo Mercadante, Fábio A. Molfetta, Cláudio N. Alves, and Albérico B. F. da Silva, *Journal of the Brazilian Chemical Society*, **14**, No. 5: 809 (2003); <https://doi.org/10.1590/S0103-50532003000500017>
28. P. Udhayakala and T. V. Rajendiran, *Journal of Chemical, Biological and Physical Sciences*, **2**, No. 1: 172 (2011); <https://jcbssc.org/api/public/getFileOld/a/47>
29. M. Salazar-Villanueva, A. B. Hernandez, E. C. Anot, J. R. Mora, J. A. Ascencio, and A. M. Cervantes, *Molecular Simulation*, **39**, No. 7: 545 (2013); <https://doi.org/10.1080/08927022.2012.754098>
30. A. N. Chibisov, *Molecular Physics*, **113**, No. 21: 3291 (2015); <https://doi.org/10.1080/00268976.2015.1017544>
31. P. Larkin, *Infrared and Raman Spectroscopy: Principles and Spectral Interpretation* (Elsevier Inc.: 2013).
32. K. S. Jeong, C. Chang, E. Sedlmayr, and D. Sülzle, *Journal of Physics B: Atomic, Molecular and Optical Physics*, **33**, No. 17: 3417 (2000); [doi:10.1088/0953-4075/33/17/319](https://doi.org/10.1088/0953-4075/33/17/319)